# Fast Edge-Based Stereo Matching and Geometric Parameters

**Payman Moallem**[↑] **and Karim Faez**[↑]

**Summary**

For an edge-based stereo matching, we establish the relationship between the search space and the geometric parameters of stereo like image resolution, CCD dimension and focal length. Moreover we show that relative displacement of the edges and disparity under consideration is effective in search space. Then, we propose a novel matching strategy for the edge-based stereo and then develop a fast algorithm with combination of the obtained matching strategy and the multiresolution technique. Considering the conventional multiresolution techniques using Haar wavelet, we show that the execution time of our algorithm is decreased more than 36%. Moreover, the matching rate and the accuracy is increased too.

## Introduction

Finding the corresponding edges is considered being the most difficult part of the edge-based stereo matching algorithm [1]. Usually, the correspondence for a feature point in the first image is obtained by searching in a predefined region of the second image, based on the epipolar line and the maximum disparity constraint [2]. The reduction of the search region can increase the performance of the matching process, in the context of the execution time and the accuracy. Traditionally, the hierarchical multiresolution techniques using wavelet transform, as the fast methods are used to decrease the search space and therefore increase the processing speed [3].
Considering the limit of the directional derivative of the disparity [4], we could restrict the search space in the edge-based stereo correspondence [5]. In this paper, we establish a relationship between the search space and the geometric parameters, like focal length, CCD dimension, image resolution and disparity under consideration. In next section, we briefly discuss the concept of DDD (the directional derivative of the disparity). Then, we establish a relationship between DDD and the displacement of feature points (like edges) in the left and right images. Considering the pdf of DDD, we already obtained a probabilistic relationship between the search space and the geometric constraint [5]. We extend those and based on the obtained relationships, suggest a fast matching strategy for an edge-based stereo. Then we develop a fast edge-based stereo matching algorithmth with multiresolution technique and our matching strategy [5][6]. Finally, we discuss about the implementation results.

## Directional Derivative of Disparity

Figure 1 shows the cameras geometry for a basic stereo system where the cameras optical axes are parallel to each other and perpendicular to the baseline connecting the two cameras L and R. $O_L$ and $O_R$ are the optical centers of the left and right camera and $O_l$ and $O_r$ are the origins of the left and right image plane. For a point P(X,Y,Z) in

[↑] E.E. Department, Amirkabir University of Technology, Tehran, Iran, {m7523903, kfaez}@aut.ac.ir

3D scene, its projections onto the left image and the right image are $p_l(x_l,y_l)$ and $p_r(x_r,y_r)$. Considering this camera geometry, it can be shown that $y_l=y_r$ and the disparity $d$ is inversely proportional to the depth Z. we have $d=bf/Z$, where $f$ is the focal length of the camera lens and $b$ is the separation of two cameras or baseline [2]. Given two points $P^1$ and $P^2$ in 3D scene, DDD can be defined as the difference in disparities divided by the cyclopean separation, where cyclopean separation is the average distance between $(p_l^1,p_r^1)$ and $(p_l^2,p_r^2)$ [7]. Therefore, we have:

$$d_2 = x_l^2 - x_r^2, \qquad d_1 = x_l^1 - x_r^1, \qquad p_c^2 = \frac{p_l^2 + p_r^2}{2}, \; p_c^1 = \frac{p_l^1 + p_r^1}{2} \tag{1}$$

With these definitions, $d_\alpha$ can be defined as [7]:

$$d_\alpha = (d_2 - d_1)/r = (d_2 - d_1)/\left\| p_c^2 - p_c^1 \right\| \tag{2}$$

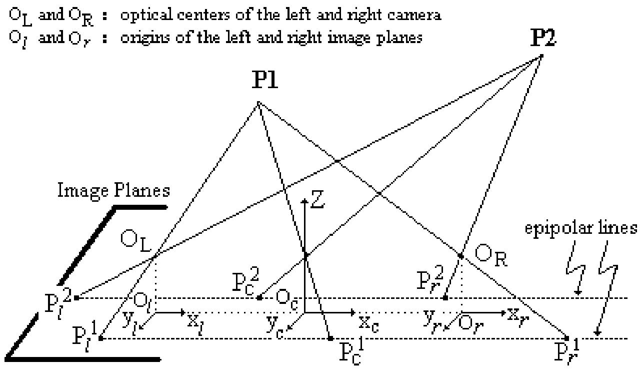


**Figure 1. Defining directional derivative of disparity in the stereo system with parallel cameras**

## DDD and the Displacements of the Edges

Suppose the feature points in the left image are non-horizontal edges in successive scan lines. We want to find their correspondences in the right image. Considering the points $P^1$ and $P^2$ in Figure 1, we define the displacement of $P^1$ and $P^2$ in the left and the right images, $\Delta x_l$, $\Delta x_r$ and $\Delta y$ as:

$$\Delta x_l = x_l^2 - x_l^1, \qquad \Delta x_r = x_r^2 - x_r^1, \qquad \Delta y_l = \Delta y_r = \Delta y = y^2 - y^1 \tag{3}$$

For the edge points in the successive scan lines, we have $\Delta y=1$, so the equation (2) can be simplified as [5]:

$$\mathrm{d}_\alpha = (\Delta x_l - \Delta x_r)/\sqrt{((\Delta x_l + \Delta x_r)/2)^2 + 1} \tag{4}$$

Suppose $x_l^1 = x_l^2$, it means $\Delta x_l=0$. Considering equation (4), we can find the upper and the lower limits of $d_\alpha$ in some ranges of $\Delta x_r$. Some results are shown in Table 1.

**Table 1. The Range of $d_\alpha$ for some values of $\Delta x_r$, in case of $\Delta x_l=0$**

| Some values of $\Delta x_r$ | -1,0,1 | -2,-1,0,+1,+2 | -3,-2,...,2,3 | -4,-3,...,3,4 |
|---|---|---|---|---|
| Range of $d_\alpha$ | $-0.89< d_\alpha<0.89$ | $-1.41< d_\alpha<1.41$ | $-1.66< d_\alpha<1.66$ | $-1.79< d_\alpha<1.79$ |

While the $\Delta x_r$ range is increased, the $|d_\alpha|$ limit is neared to 2, which violates the uniqueness constraint in the stereo system [5]. For other values of $\Delta x_l$ and $\Delta x_r$, the ranges of $d_\alpha$ can be computed. Some results for $\Delta x_l=+1$ are shown in Table 2. The other cases ($\Delta x_l=-1$, $\Delta x_l=+2$ and $\Delta x_l=-2$) can be simply computed. In Table 2, $d_\alpha$ is +2 in the case of $\Delta x_l=+1$ and $\Delta x_r=-1$. Since the upper limit of $d_\alpha$ is 2, so there is no need to decrease $\Delta x_r$ lower than -1. On the other hand, while $\Delta x_r$ can be increased toward positive infinity, then $d_\alpha$ is also neared to -2, which is the lower limit of $d_\alpha$ [5].

**Table 2. The Range of $d_\alpha$ for some values of $\Delta x_r$, in case of $\Delta x_l=+1$**

| Some values of $\Delta x_r$ | 0,1,2 | -1,0,1,2,3 | -1,0,1,2,3,4 | -1,0,1,2,3,4,5 |
|---|---|---|---|---|
| Range of $d_\alpha$ | $-.55< d_\alpha<.89$ | $-.89< d_\alpha<2.0$ | $-1.11< d_\alpha<2.0$ | $-1.26< d_\alpha<2.0$ |

## DDD Ranges and Disparity Values

In the previous section, the DDD range was related to the $\Delta x_l$ value and the $\Delta x_r$ range. When $\Delta x_l$ is known, the $\Delta x_r$ range can be selected if the range of $d_\alpha$ is already determined. We will show that the range of $d_\alpha$ is a probabilistic phenomenon and it is dependent on the stereo system parameters and the disparity value [6]. The pdf of DDD for a point ($x_l$,y) in the left image with disparity *d* may be found by mapping DDD of the equation (2), into a tangent direction at [X,Y,Z] in the 3D space of the scene, and using the relationship to transform the pdf of the scene coordinate tangent to the pdf of DDD [4]. Performing these calculations and approximating the results for simplification results in equation (5). The general shape of this pdf is similar to a Gaussian function. Moreover this pdf depends explicitly on the disparity under consideration (*d*) and the focal length of the cameras (*f*), or equivalently on the depth and the inter-camera baseline (since *f/d=Z/b*).

$$P_{d_a}(d_a) = \frac{f/d}{2(1+(f/d)^2 . {d_\alpha}^2)^{3/2}} \qquad (5)$$

As an example, consider CIL images database, Calibrated Imaging Laboratory at CMU, Carnegie Mellon University [8]. Some geometric parameters of the CIL images are listed in Table 3. Therefore the focal length of the CIL is about 2478 pixels. Figure 2 shows the pdf's for various disparity as a function of DDD values. These functions have some sharp peaks near zero DDD and become wider when disparity increases.

**Table 3. Some of the CIL Geometric Parameters**

| | |
|---|---|
| Horizontal cells in CCD Array | 576 |
| Horizontal pixels in computer frame buffer | 576 |
| Distance between sensor elements (mm) | 2.3e-2 |
| Focal length (mm) | 57 |

Assume the range of $d_\alpha$ is $Rd_\alpha=\{d_\alpha^L < d_\alpha < d_\alpha^H\}$, therefore the $P(d_\alpha \in Rd_\alpha)$ can be obtained by integrating equation (6) over $Rd_\alpha$ as:

$$P(d_a \in Rd_a) = \int_{d_\alpha^L}^{d_\alpha^H} P_{d_a}(d_a).d(d_a) \qquad (6)$$

We are interested in finding the maximum of the disparity (or $d_{max}$) so that $P(d_\alpha \in Rd_\alpha) > P_{proper}$. $P_{proper}$ as a proper value of $P(d_\alpha \in Rd_\alpha)$ is selected near to 1. For the above example, $P_{proper}$ =0.995 is a suitable value [6].

**Table 4. $d_{max}$ for some values of $\Delta x_r$ ,in case of $\Delta x_l$=0**

| Some values of $\Delta x_r$ | -1,0,1 | -2,-1,0,1,2 | -3,-2,1,0,1,2,3 | -4,-3,-2,1,0,1,2,3,4 |
|---|---|---|---|---|
| $d_{max}$ | 230 | 360 | 420 | 450 |

Table 4 and 5 show the relations between $d_{max}$ and $\Delta x_r$ in the case of $\Delta x_l$=0 and +1 by context $P(d_\alpha \in Rd_\alpha)$>0.995, for other values of $\Delta x_l$, the computations are similar.

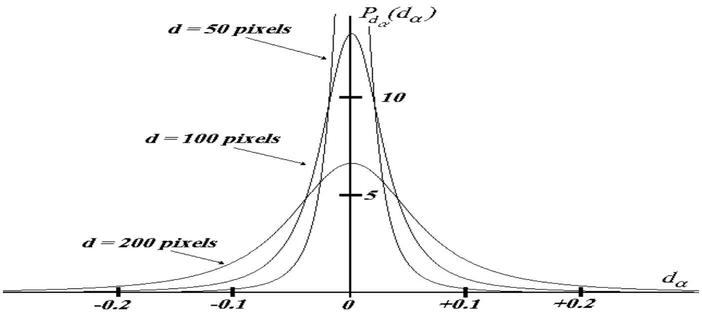


**Figure 2. Graph of $Pd_\alpha$ vs. $d_\alpha$ for three different disparities d=50, d=100 and d=200 pixels for the CIL images database at CMU**

## Fast Algorithm

Our matching algorithm has two stages: edge extraction and edge matching. The edge extraction stage consists of identifying non-horizontal thinned edges, extracted in the left and right images. At first, two images are convolved with a proper gradient mask. We use gradient of Gussian in x direction, with a size of 5×5. The filter response at corresponding point has to exceed a pre-defined threshold and has to obtain a local maximum [1]. Then, the extracted thinned edges are classified into two types, positives and negatives, depending on their slopes with respect to the x direction. In the matching, we use successive connected edge sets.

**Table 5.** $d_{max}$ **for some values of** $\Delta x_r$ **,in case of** $\Delta x_l$**=+1**

| Some values of $\Delta x_r$ | 0,1,2 | -1,0,1,2,3 | -1,0,1,2,3,4 | -1,0,1,2,3,4,5 |
|---|---|---|---|---|
| $d_{max}$ | 170 | 290 | 340 | 380 |

Some connected edge points in the left image can be grouped together as some sets that we call *successive connected edges* (SCE) sets. Each SCE set $\Psi$ consists of $n$ successive edges, $\Psi = \{ p^l_1, p^l_2, p^l_3 ....., p^l_n\}$. Its coordinates and type identify each edge point as $p^l_k$, $p^l_k = (x^l_k , y^l_k$ , type). The set $\Psi$ is said a *successive connected edges* set if these three conditions are met:

**1**-The types of all $p^l_k$ are the same. **2**-The successive $p^l_k$'s are in successive scan lines. Therefore we have, $y^l_{k+1} - y^l_k = 1$. **3**-The absolute difference between x values of two successive points is less than 3, so we have, $x^l_k - x^l_{k+1} = \{-2,-1,0,+1,+2\}$.

In the matching stages of each SCE in the left image, our algorithm has two phases.

**Phase one:** At the first point of a SCE, we use the conventional multiresolution technique using Haar wavelet [3] to reduce the search region. We use three levels of Haar wavelet (original+two lower resolution). We use the normalised cross correlation (NCC) with the window size of 11×11, 13×13 and 15×15 for the coarse, medium and fine level. In the coarsest level, the search space is selected by considering the maximum of the disparity. At the higher resolution levels, the search space is cut around each found maximum correlation location in the previous level, ±7 pixels along the epipolar line. At the highest resolution, only the similar edges on the epipolar line of other image are examined.

Considering the relationship between disparities, $\Delta x_l$ and $\Delta x_r$, we showed that the search region could be reduced. If the disparity search range could be automatically reduced to an effective range (about 10 pixels or less), then several local maximum would stay out of the selection process and therefore, the disparities found would be correct, even if the size of the matching block is small [9]. Therefore, we can use NCC with a window size of even 3×3 in the restricted search region.

**Phase two:** If we can find the correspondence of that point in the second image, we use restricted search region based on one of the computed tables, for other SCE points. If there is only one similar edge point in the restricted search region, that point is selected without any further examination. If not, NCC with the window size of 3×3 is examined. If we can not find the correspondence, the algorithm finds the first point of the next connected edges in the left image and then goes to phase one.

## Implementation Results

For comparing the results of the execution time and accuracy, we choose a multiresolution method as the reference that is based on the first phase of the proposed algorithm. The feature points used in the reference algorithm and in our algorithm are non-horizontal edge points. We implemented and tested the proposed algorithm and the reference one for CIL Castle images at CMU [8]. One pair is shown in Figure 3. The maximum of the disparity in these two images is around 110 pixels, which is the highest disparity among this set. We consider the disparity range between 0 to 110 pixels. Some results are shown in Figure 3. For other stereo images in that set, the performances are similar.

**(a) (b) (c) (d)**

**Figure 3. The Castle stereo images as test images, (a) and (b) are left and right image, (c) and (d) are the disparity maps for the reference and proposed algorithm.**

The feature point extraction stage found 4963 non-horizontal edges. The results of matching are shown in Table 6, which tabulates the number of the matched points, the error points, the execution time and finally the speed up. The values of the speed up are with respect to the reference algorithm. The codes of the algorithms were written by Watcom C and implemented by a PC under Windows operating system, with a Pentium II 450 MHz processor. The execution time of the feature point extraction stage is about 0.11 seconds. The matching stage is executed in 0.66 seconds for our algorithm and 1.11 seconds for the reference one. The execution time of our algorithm is about 1.58 times faster than the reference one and moreover, the error is also decreased. Moreover, the matched points are a little higher than the reference one.

**Table 6. The implementation results of the algorithm on Castle stereo image**

| Algorithm | Matched Points | Error Points | Execution Time | Speed Up |
|---|---|---|---|---|
| Reference | 1995 | 35 | 1.22 Sec | 1 |
| Proposed | 2090 | 22 | 0.77 Sec | 1.58 |

## Conclusion

We proposed the fast edge-based stereo matching algorithm based on the new search space reduction and the traditional multiresolution algorithm using Haar wavelet. Our proposed algorithm is executed 1.58 times faster and the error and the matching failed are also lower. Therefore this algorithm can be used in some fast edge-based stereo matching applications, like stereo robot vision.

## References


[1] T. Frohlinghaus, J.M Buhmann, "Real-Time Phase-Based Stereo for Mobile Robot", in Proc. EUROBOT96, pp.178-185, 1996.

[2] E. Trucco, A. Verri, Introductory Techniques for 3D Computer Vision, Prentice Hall, 1998.

[3] S. Brandt, J. Heikkonen, "Multi-Resolution Matching of Uncalibrated Images utilizing Epipolar Geometry and its Uncertainty", in Proc. ICIP2001, Vol. 2, pp. 213-216, 2001.

[4] C.Stewart, R.Flatland, K.Bubna,"Geometric Constraints and Stereo Disparity Computation", Int. Jour. of Computer Vision, Kluwer Academic Publisher, Vol. 20, No 4, pp. 143-168, 1996.

[5] P. Moallem, K. Faez, "Search Space Reduction in the Edge Based Stereo Correspondence", in Proc. VMV2001, 2001.

[6] P. Moallem, K. Faez, J. Haddadnia, "Reduction of the Search Space Region in the Edge-Based Stereo Correspondence", in Proc. ICIP2001, pp. 149-152, 2001.

[7] Z. Li, G. Hu, "Analysis of Disparity Gradient Based Cooperative Stereo", IEEE Trans. on Image Processing, Vol. 5, No 11, pp. 1493-1506, Nov. 1996.

[8] CIL Images Dataset at http://www-2.cs.cmu.edu/~cil/cil-ster.html.

[9] M.A. Torres, A.R. Guesalga, "Confidence Factor and Adaptive Disparity Range for Reliable 3D Reconstruction", Computer Intelligence for Modeling & Automation, M. Mohammadian, IOS Press, 1999.